

## Supporting Information for

Modifications in the T arm of tRNA globally determine tRNA maturation, function and cellular fitness

**Sarah K. Schultz**<sup>1,2</sup>, **Christopher D. Katanski**<sup>3</sup>, **Mateusz Halucha**<sup>3</sup>, **Noah Pena**<sup>4</sup>,  
**Richard P. Fahlman**<sup>5</sup>, **Tao Pan**<sup>3</sup>, **Ute Kothe**<sup>\*1,2</sup>

<sup>1</sup> *Department of Chemistry, University of Manitoba, 144 Dysart Road, Winnipeg, R3T 2N2, MB, Canada*

<sup>2</sup> *Alberta RNA Research and Training Institute (ARRTI), Department of Chemistry and Biochemistry, University of Lethbridge, 4401 University Drive, T1K 3M4 Lethbridge, AB, Canada*

<sup>3</sup> *Department of Biochemistry & Molecular Biology, University of Chicago, Chicago, IL 60637, USA*

<sup>4</sup> *Department of Molecular Genetics and Cell Biology, University of Chicago, Chicago, IL 60637, USA*

<sup>5</sup> *Department of Biochemistry, University of Alberta, 474 Medical Sciences Building, University of Alberta, Edmonton, T6G 2H7, AB, Canada*

## Corresponding author:

Ute Kothe, Department of Chemistry, University of Manitoba, 144 Dysart Road, Winnipeg, R3T 2N2, MB, Canada, 204-474-9265, [ute.kothe@umanitoba.ca](mailto:ute.kothe@umanitoba.ca)

**This PDF file includes:**

SI Methods

Figures S1 to S15

Table S1

Legends for Datasets S1 to S5

SI References

**Other supporting materials for this manuscript include the following:**

Datasets S1 to S5

## **SI Methods**

### **Chemicals and reagents**

Unless otherwise stated, all reagents were purchased from ThermoFisher Scientific. All oligonucleotides were purchased from Integrated DNA Technologies (IDT) and are listed in Table S1.

### ***E. coli* strains**

All *E. coli* wildtype and single knockout strains are BW25113 derivatives from the Keio Collection (1). To construct the  $\Delta trmA\Delta truB$  double knockout, the FLP recognition target (FRT)-flanked kanamycin resistance cassette was removed from the Keio  $\Delta trmA$  strain, and the *truB* gene was subsequently replaced by a FRT-flanked kanamycin resistance cassette using  $\lambda$  Red recombinase (2). All gene deletions were confirmed by colony PCR using primers specific for the kanamycin resistance cassette ( $k_1/k_2$ ) and primers targeting the locus upstream and downstream of the deleted gene (Table S1).

### ***E. coli* phenotypic microarray screening, cell growth assays and co-culture competition assays**

Biolog phenotypic microarray screening was performed by Microbe Inotech (St. Louis, Missouri) as described (3). One biological replicate was performed for each the BW25113 wildtype strain and the  $\Delta trmA\Delta truB$  strain. To follow-up on potentially interesting growth conditions, *E. coli* growth assays were performed as described below.

At least four biological replicates for each strain were grown overnight in LB media without antibiotic (for the BW25113 wildtype strain) or with 50 µg/mL kanamycin (knockout strains). Cells were resuspended in the appropriate fresh media (LB, Bochner rich, or Bochner minimal media as indicated (3)) lacking kanamycin and diluted to an OD<sub>600</sub> of 0.1 for liquid growth or to an OD<sub>600</sub> of 1 followed by a 10-fold dilution series for agar spot plate assays. Liquid 96-well plate cultures were incubated at 37°C for 48 hours with continuous shaking in an Eon BioTrek 96-well plate reader and absorbance at 600 nm was recorded every 15 minutes. The OD<sub>600</sub> values for each biological replicate were averaged and plotted versus time with error bars representing the standard error of the mean (SEM).

Competition assays were performed similarly as reported in (4). In brief, equal concentrations of BW25113 and *ΔtrmAΔtruB* were mixed and grown at 37°C with shaking. Every 24 hours, the ratio of kanamycin resistant (knockout) colonies was compared to the total number of colonies by plating on LB agar plates with and without 50 µg/mL kanamycin and cultures were diluted 10x10<sup>6</sup> in fresh media to begin the next cycle.

### **Total RNA extractions for tRNAseq, Northern blotting, and primer extension**

Cells were grown overnight in LB medium (wildtype) including 50 µg/mL kanamycin (knockout strains) from single colonies. Cultures were centrifuged and resuspended in fresh LB media or LB including 2% (w/v) sodium formate as indicated. Cultures (50 mL) were started at an OD<sub>600</sub> of 0.1 and grown until reaching an OD<sub>600</sub> of 0.3-0.4, when 15 mL culture was harvested and shock frozen. RNA extractions were accomplished under acidic conditions (pH <5) to preserve the aminoacyl bond using



TRIzol (Invitrogen), following the manufacturer's instructions. In brief, cells were resuspended in 3 mL TRIzol, followed by the addition of 0.6 mL chloroform. After centrifugation (30 minutes, 6000 g), the aqueous layer was removed and ethanol precipitated several times. Purified RNA was resuspended in 10 mM NaOAc (pH 4.8) and stored at -80 °C. Concentrations were determined using UV spectrometry (NanoDrop 2000c).

### **MSR-tRNA-seq for tRNA abundance, aminoacylation, and certain modifications**

During MSR-tRNAseq, the 3' ribose of uncharged tRNA is oxidized leading to  $\beta$ -elimination of the 3' adenine of the tRNA whereas the terminal 3' adenine is protected in aminoacylated tRNA. After Illumina sequencing, comparison of sequences ending in 3' CC (deacylated) to 3' CCA (aminoacylated) allows for quantification of the aminoacylation level for individual tRNA isoacceptors while also providing information about relative tRNA abundance and modification content (5, 6). Library preparation, MSR-tRNA-seq and data analysis were conducted as previously published (6). Three biological replicates were sequenced for each strain and condition. The *E. coli* tRNA reference was obtained from Genomic tRNA database (7). Modification was identified by mutation and deletion signatures that were generated by Superscript IV read-through. Source codes for all custom scripts are available on GitHub (<https://github.com/ckatanski/CHRIS-seq>).

### **Calculations for tRNA variable loop stability for tRNA<sup>Leu</sup> isoacceptors**

Free energies for each tRNA variable loop sequence were calculated using the Predict a Secondary Structure web server

(<https://rna.urmc.rochester.edu/RNAstructureWeb/Servers/Predict1/Predict1.html>).

### **Northern blotting for tRNA thiolation**

The fraction of thiolated tRNAs was compared to non-thiolated tRNAs by separating RNA on a gel containing a phenylmercury compound that slows the migration of thiolated tRNAs. Specifically, 5 µg total RNA was separated on a 20 µM [(N-acryloylamino)phenyl]mercuric chloride (APM, Toronto Research Chemicals) 7 M urea 12% polyacrylamide gel (8). To reduce APM-thiol linkages, APM gels were soaked in 0.2 M β-mercaptoethanol for one hour prior to transfer. RNA was transferred to a nylon membrane (Amersham Hybond-XL) at 23 V for 7 minutes using a Trans-Blot Turbo Transfer System (Bio-Rad). Following transfer, blots were crosslinked twice at 1200 mJ. Northern blotting was performed similarly as described in (9) using biotinylated probes (Table S1), which were detected after incubation with 120 ng/mL streptavidin-HRP (Genscript) in hybridization buffer for one hour. To detect chemiluminescence, a solution containing 375 ng/mL luminol, 55 ng/mL p-coumaric acid, and 0.1% (v/v) hydrogen peroxide was applied to the blot immediately prior to imaging with a FluorChem Q imager (Cell Biosciences). Densitometry was performed using ImageJ.

### **Primer extension to detect acp<sup>3</sup>U47 modification**

Since the bulky acp<sup>3</sup>U47 mutation causes reverse transcription stops for a reverse transcriptase with a low processivity, we used a primer extension assay to

compare the relative abundance of  $\text{acp}^3\text{U47}$  between *E. coli* strains lacking *trmA* and/or *truB* genes and the wildtype strain. Reverse transcriptions were performed by first annealing 1700 ng of total RNA to 3 pmol Cy5-labeled  $\text{tRNA}^{\text{Phe}}$  reverse transcription primer by heating to 65 °C and cooling to 47 °C. The RNA-primer mixture was then added to a reaction mixture containing final concentrations of 136 ng/ $\mu\text{L}$  total RNA, 240 nM Cy5-labeled reverse transcription primer, 0.4 mM dNTPs, and 8 mM DTT, in 1X AMV reverse transcription buffer. After pre-heating to 47°C, AMV reverse transcriptase (New England Biolabs) was added to a final concentration of 0.4 U/ $\mu\text{L}$  and incubated at 47 °C for 45 minutes. The reaction was ended by heating to 70°C for 15 minutes. Samples (7  $\mu\text{L}$  of the reverse transcription reaction) were analyzed on an 8 M urea 8% polyacrylamide sequencing gel in TBE which was preheated to 50°C at 50 W until the bromophenol blue dye front was halfway down the gel. Gels were imaged on a Typhoon 5 scanner. The intensity of the bands corresponding to reverse transcription stop at position 47 was normalized to the band corresponding to a reverse transcription stop at position 37 for each strain (ratio 47/37).

### **Total RNA sequencing**

Cells were grown overnight in LB medium (wildtype) including 50  $\mu\text{g/mL}$  kanamycin (knockout strains) from single colonies. Cultures were centrifuged and resuspended in LB including 2% (w/v) sodium formate. Cultures (50 mL) were started at an  $\text{OD}_{600}$  of 0.1 and grown until reaching an  $\text{OD}_{600}$  of 0.3-0.4, when 15 mL culture was harvested and shock frozen. As TRIzol extractions from *E. coli* cells are known to be biased towards the extraction of small RNAs (10), to promote proportionate presence of mRNAs of all sizes, *E. coli* cells were first resuspended in 300  $\mu\text{L}$  of a cell opening

buffer (100 mM Tris, 10 mM EDTA, 0.5% SDS, 286 mM  $\beta$ -mercaptoethanol) containing 10 mg/mL lysozyme, 0.1 U/ $\mu$ L DNase I, and 0.1 U/ $\mu$ L RiboLock RNase inhibitor (ThermoFisher) and incubated at 37°C for 5 minutes. Subsequently, Proteinase K (ThermoFisher) was added to a final concentration of 0.5 mg/mL, and lysates were incubated at 50°C for 10 minutes. RNA extractions were performed as described above. Further DNase treatment, RNA quality analysis by TapeStation and DNA/RNA Qubit, library preparation, strand-specific Illumina sequencing with a HiSeq4000, and data analysis were performed by Azenta. In brief, reads were trimmed with Trimmomatic v.0.36 and trimmed reads were mapped to the *E. coli* BW25113 genome using Bowtie2 v.2.2.6. Unique gene hit counts were calculated by using featureCounts from the Subread package v.1.5.2 and gene expression was compared between *E. coli* strains using DESeq2.

### **Bioorthogonal noncanonical amino acid tagging (BONCAT)**

*E. coli* pre-cultures were grown overnight in the appropriate antibiotic in 5 mL LB medium. Stationary-phase cells were harvested, washed, and resuspended in M9 minimal media containing 1.75% sodium formate, and 50 mL cultures were grown at 37°C starting at an OD<sub>600</sub> of 0.1. When cultures reached an OD<sub>600</sub> of ~0.3, L-azidohomoalanine (L-AHA, Sigma) was added to a final concentration of 1 mM. L-AHA is incorporated into newly synthesized proteins instead of L-methionine allowing for labelling with a rhodamine dye. Twenty minutes and 40 minutes post-L-AHA addition, 0.5 OD<sub>600</sub> units of cells were harvested, fixed with 3% (v/v) formaldehyde, washed into PBS, and stored at -20 °C. Cell opening and fluorescent labeling of L-AHA-containing proteins with DBCO-PEG4-Carboxyrhodamine 110 (Click Chemistry Tools) were

performed as described (11). Proteins were purified using chloroform-methanol extraction and resuspended in 6.4 M urea and 200 mM DTT; total protein concentration was determined by UV spectrometry:

$$\text{Concentration (mg/mL)} = (1.55 \times A_{280}) - (0.76 \times A_{260})$$

Protein samples were denatured at 65°C prior to analyzing 5 µg total protein on a 12% SDS-PAGE. Labeled proteins were detected using the 488 nm laser on a Typhoon 5 Imager (Cytiva). To confirm equal loading, gels were stained with Coomassie. Relative global translation for each strain was estimated by densitometry (ImageJ).

### **Proteome comparison by mass spectrometry**

Four biological replicates of each strain were grown at 37 °C in LB media containing 2% (w/v) sodium formate until reaching an OD<sub>600</sub> between 0.3 and 0.4. Following harvesting, cells were resuspended in 8 M urea containing SDS loading buffer lacking any colored dyes and 0.3 OD<sub>600</sub> units of each sample were analyzed on a 12% SDS PAGE and stained with Coomassie.

Each lane was excised and subsequently cut into 14 equal bands and each gel fraction was subjected to in-gel tryptic digestion as previously described (12) and the resulting peptides were dried and resuspended in 60 L of 0.2% formic acid in 5% acetonitrile (ACN). Digested peptides were analyzed by LC-MS/MS using a ThermoScientific Easy nLC-1000 in tandem with a Q-Exactive Orbitrap mass spectrometer. Each sample (5 µL) was resolved using a 120 min gradient [0%–45% Buffer B; Buffer A (0.2% formic acid in 5% ACN); Buffer B (0.2% formic acid in 100% ACN)] on a 2 cm Acclaim 100 PepMap Nanoviper C18 trapping column in tandem with

a Thermo EASY-Spray column (PepMap® RSLC, C18, 3  $\mu$ m, 100 Å, 75 m  $\times$  150 mm). For data-dependent analysis, full scans were acquired at 35000 resolution at a range of 400–200 m/z while 17500 resolution was used for MS/MS scans. Only top 15 ions with +2 and +3 charges were selected for MS/MS with 10 s dynamic exclusion applied to prevent continuous reanalysis of abundant peptides. Following data acquisition, raw data files were compiled for each gel lane and searched with Proteome Discoverer 1.4's SEQUEST search algorithm using the reviewed, non-redundant *E. coli* complete proteome retrieved from UniProtKB. The search parameters and quantification were as previously described (13).

Proteins were considered to be significantly different in each knockout compared to the wildtype for  $p$  values  $<0.05$  determined by a two-tailed paired Student's  $t$  test. To address proteins that were not identified in any wildtype replicates (fold change = division by zero) or not identified in a knockout (fold change = 0), a small value (0.1) was added to each value for the purpose of determining fold change relative to wildtype (Dataset S4). Significantly enriched GO terms in each dataset were determined using PANTHER GO biological complete annotation set and by Fisher's Exact test, correcting for False Discovery Rate (14) using the set of proteins detected by mass spectrometry as the background. Redundant GO terms were removed using REVIGO (15).

### **Codon analysis**

Using individual gene sequences for *E. coli* K-12 MG1655 obtained from the EcoCyc database (16), codon frequencies for each coding sequence were calculated using the Sequence Manipulation Suite: Codon Usage tool (17). Codon frequencies for each gene were compared to the *E. coli* K-12 codon usage table (Eecoli.cut (18)) to

determine the relative codon usage for each examined gene compared to overall *E. coli* codon usage:

$$\text{Relative codon usage (specific gene)} = \frac{\text{freq. per 1000 for codon in specific gene}}{\text{freq. per 1000 for codon in } E. coli \text{ genome}}$$

### **Translation reporter assays to examine codon-specific translation**

BW25113 wildtype,  $\Delta trmA$ ,  $\Delta truB$ , and  $\Delta trmA\Delta truB$  strains were transformed with reporter plasmids carrying an arabinose-inducible fluorescent transcriptional cassette encoding superfolder green fluorescent protein (sfGFP) followed by mCherry fluorescent protein (kind gift of Assaf Katz, Universidad de Chile, Santiago, Chile) (19). Each reporter contains a set of four tandem repeats of a codon following the third sfGFP codon, such that sfGFP expression relies on translation of the four repeated codons. To account for small differences in translation between strains, plasmid S1 was used as a control, which lacks any additional codons in sfGFP.

sfGFP and mCherry fluorescence was determined similarly as previously described (19). In short, overnight cultures were diluted 1:20 to an OD<sub>600</sub> of ~0.1 and grown in LB medium supplemented with 100 µg/mL ampicillin until reaching an OD<sub>600</sub> of 0.4-0.6. At this point, cells were diluted 1:4 into fresh LB medium containing a final concentration of 100 µg/mL ampicillin and 0.4% (w/v) arabinose in black, optical bottom 96 well plates and grown at 37 °C with shaking at 100 rpm. Two- and three-hours post-induction, OD<sub>600</sub>, sfGFP fluorescence (excitation: 480 nm, emission: 515 nm), and mCherry fluorescence (excitation: 587 nm, emission: 610 nm) were measured using a FlexStation 3 plate reader (Molecular Devices). sfGFP/mCherry ratios for each test

codon were normalized to the sfGFP/mCherry ratio of plasmid S1 for the respective strain:

$$sfGFP/mCherry \text{ ratio relative to control} = \frac{sfGFP_{test \text{ codon}}/mCherry_{test \text{ codon}}}{sfGFP_{S1}/mCherry_{S1}}$$

For each codon, translation between strains was compared using two-way ANOVA. Significant differences ( $p < 0.05$ ) between strains are indicated.

### **Sec-tRNA<sup>Sec</sup> mediated UGA readthrough reporter assay**

To prepare a dual luciferase reporter for measuring selenocysteine insertion sequence-directed UGA readthrough that is suitable for expression within kanamycin-resistant and DE3-lacking BW25113 knockout strains, pTrc99a-fluc-*fdhF*130-179UGA-rluc was prepared by PCR amplification and ligation of the DNA sequence encoding the Fluc-FdhF-Rluc fusion protein within pET24-fluc-*fdhF*130-179UGA-rluc (20) (kind gift from Marina Rodnina, Max Planck Institute for Multidisciplinary Sciences, Göttingen, Germany). To account for subtle differences in canonical translation between strains, site-directed mutagenesis was used to construct the control plasmid, pTrc99a-fluc-*fdhF*130-179UUC-rluc, which encodes a UUC Phe codon in place of the UGA Sec codon. Plasmids were transformed into BW25113 wildtype,  $\Delta trmA$ ,  $\Delta truB$ , and  $\Delta trmA\Delta truB$  strains.

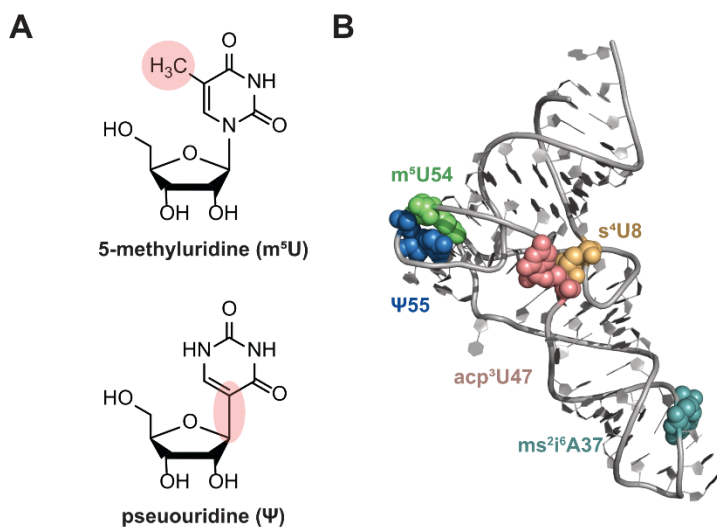
To determine the proportion of UGA readthrough in each strain, cultures were grown at 37 °C with shaking, starting at an OD<sub>600</sub> of ~0.1 in LB media supplemented with 50 µM sodium selenite. At an OD<sub>600</sub> between 0.5-0.7, fusion protein expression was induced with 1 mM isopropyl β-D-1-thiogalactopyranoside (IPTG). Following 30



minutes of growth, 0.1 OD<sub>600</sub> of cells were harvested, opened by lysozyme, and firefly and *Renilla* luciferase were measured using the Dual-Luciferase® Reporter Assay System (Promega) as per the manufacturer's instructions with a Spectramax i3 plate reader (Molecular Devices). Recoding efficiency for each strain was calculated using the following formula:

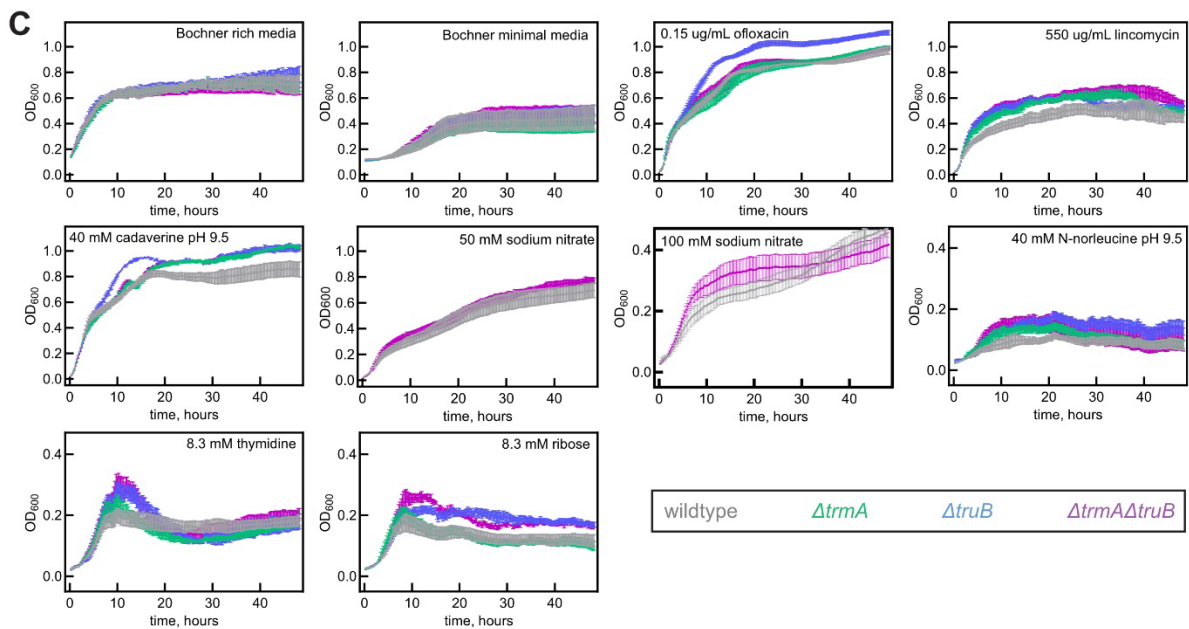
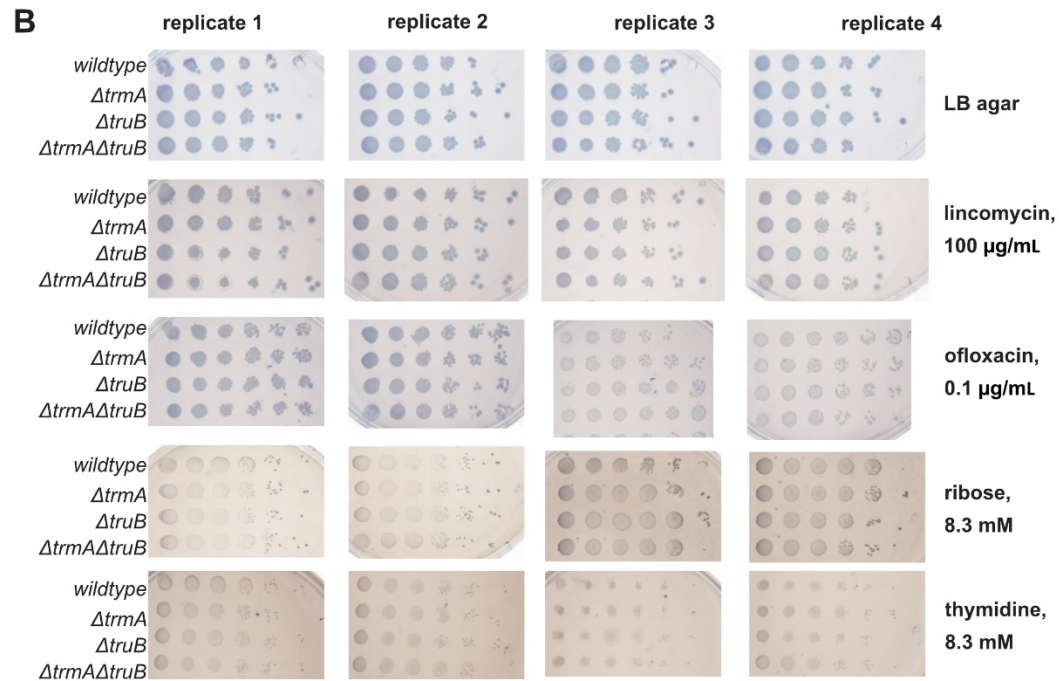
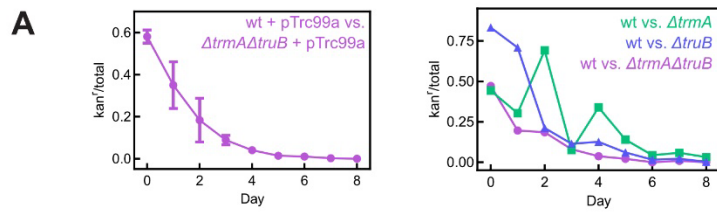
$$\% \text{ readthrough} = \frac{Rluc_{UGA}/Fluc_{UGA}}{Rluc_{UUC}/Fluc_{UUC}} \times 100\%$$

## SI Figures S1 to S15

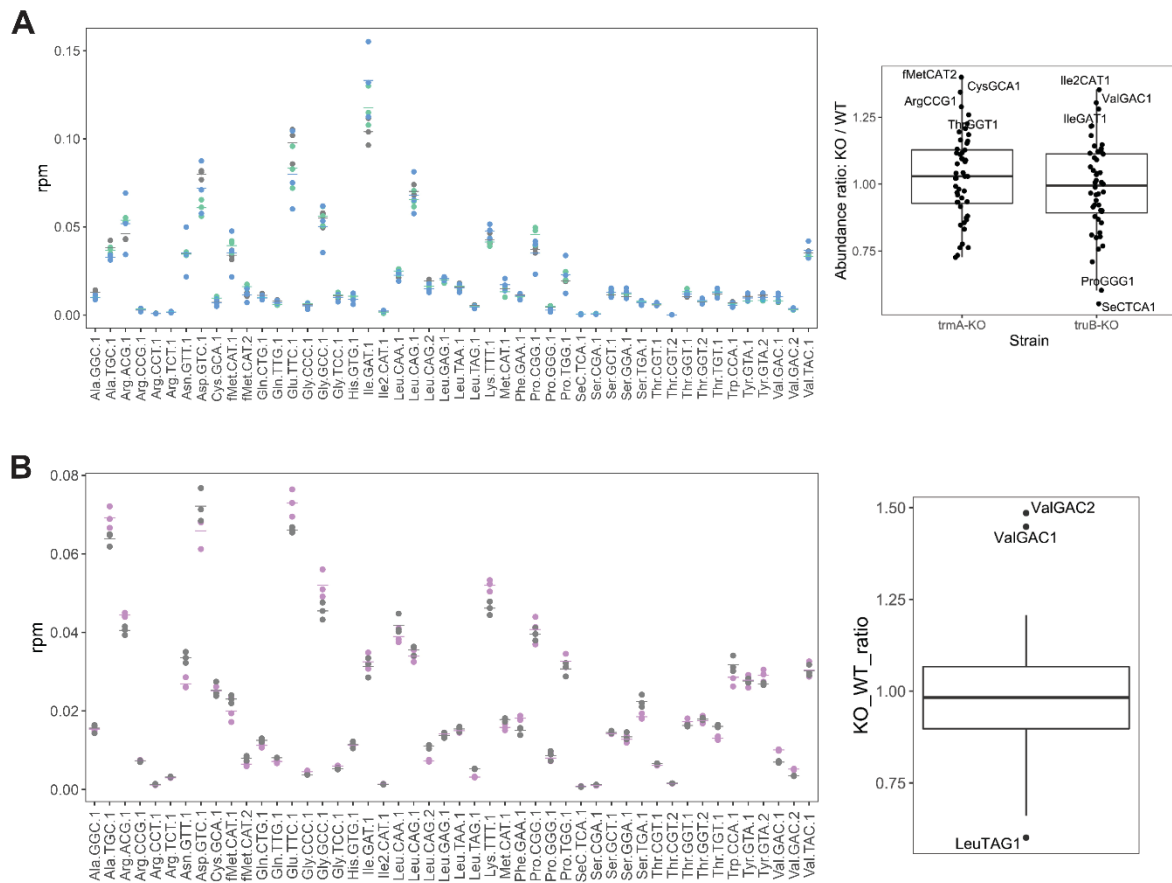


**Figure S1. Structures and location of  $m^5U54$  and  $\Psi55$ .** (A) Chemical structures of  $m^5U$  (top) and  $\Psi$  (bottom) nucleosides. The region of the modification is highlighted in red. (B) Location of  $m^5U54$  (green spheres),  $\Psi55$  (blue spheres),  $s^4U8$  (yellow spheres),  $acp^3U47$  (pink spheres), and  $ms^2i^6A37$  (teal spheres) within the crystal structure of unmodified *E. coli* tRNA<sup>Phe</sup> (PDB 3L0U) (21).



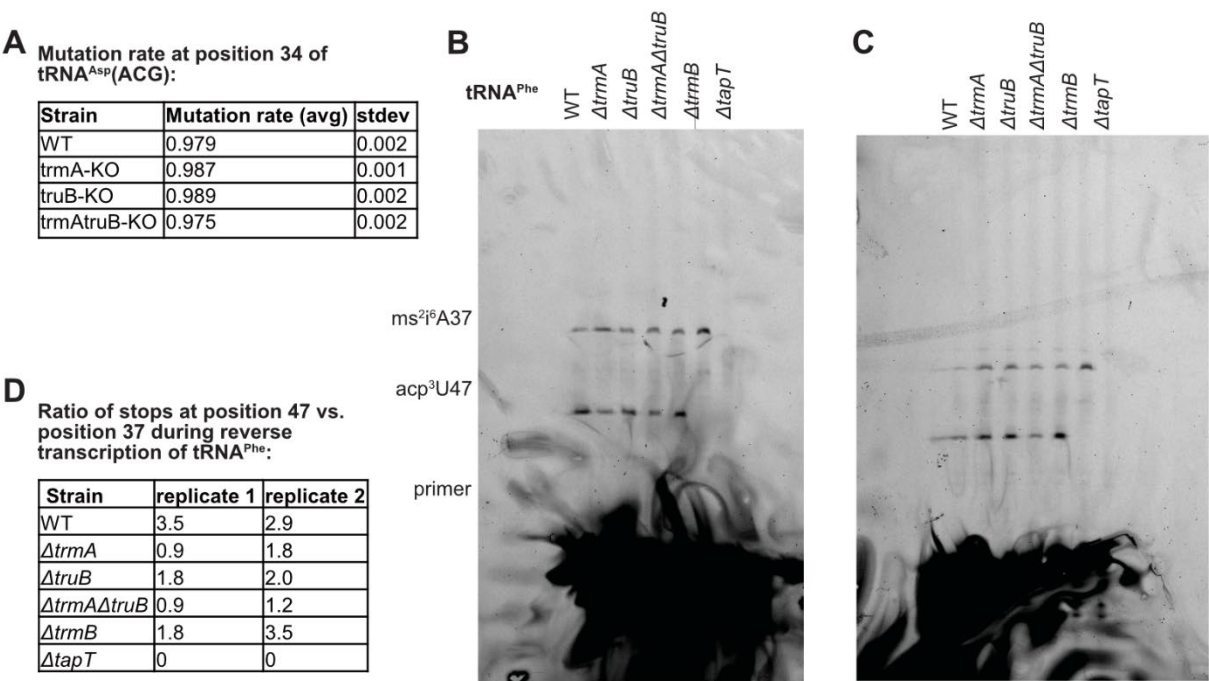


**Figure S2. Deletion of *trmA* and/or *truB* decreases cellular fitness in co-culture competition assays but does not result in growth defects in several stress conditions.** **(A)** The double  $\Delta trmA\Delta truB$  strain is outcompeted the BW25113 wildtype strain during co-culture competition assays in LB media. Equal proportions of the wildtype and  $\Delta trmA\Delta truB$  or single knockout strain carrying empty pTrc99a plasmid (left; n = 3, error bars represent standard deviation) or lacking plasmid (right; n = 1) were mixed and the proportion of kanamycin-resistant colonies (knockout strains) were compared to the total number of colonies grown on LB plates lacking antibiotic every 24 hours. **(B)** Spot plate assays comparing the growth of  $\Delta trmA$ ,  $\Delta truB$ ,  $\Delta trmA\Delta truB$ , and the BW25113 wildtype strain on agar plates containing LB agar (top) or LB agar plus 100  $\mu\text{g/mL}$  lincomycin, 0.1  $\mu\text{g/mL}$  ofloxacin, or Bochner minimal media containing 8.3 mM thymidine or 8.3 mM ribose (bottom). Plates were imaged after 16-24 hours of growth at 37°C. Four biological replicates of each strain were performed for each condition. **(C)** Growth curves for  $\Delta trmA$ ,  $\Delta truB$ ,  $\Delta trmA\Delta truB$ , and BW25113 wildtype strains in different conditions. LB media was used for all stress conditions, except for N-norleucine, thymidine, and ribose, in which Bochner minimal media was used. At least four biological replicates were performed for each curve.

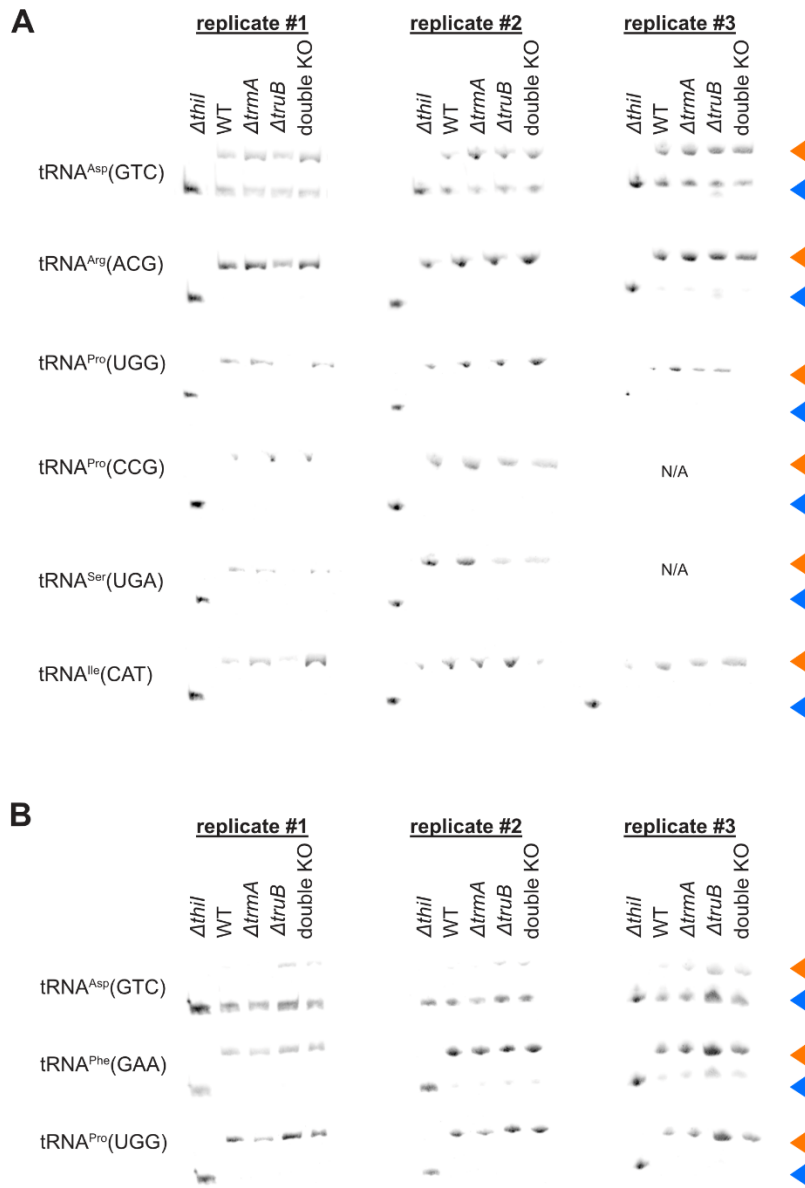


**Figure S3. Global tRNA abundance does not change in the absence of *trmA* and/or *truB* observed by RNAseq.** Reads per million (rpm) counted for each tRNA species in the wildtype (grey) compared to in single  $\Delta trmA$  (green) and  $\Delta truB$  (blue) knockout (KO) strains **(A)** or wildtype (grey) and the double  $\Delta trmA\Delta truB$  strain (purple) **(B)**. rpm values for each replicate are depicted as dots and lines represents averages for three replicates. Box plots (right side of each panel) depict the global relative

abundance for each tRNA species in each knockout strain in comparison to wildtype.



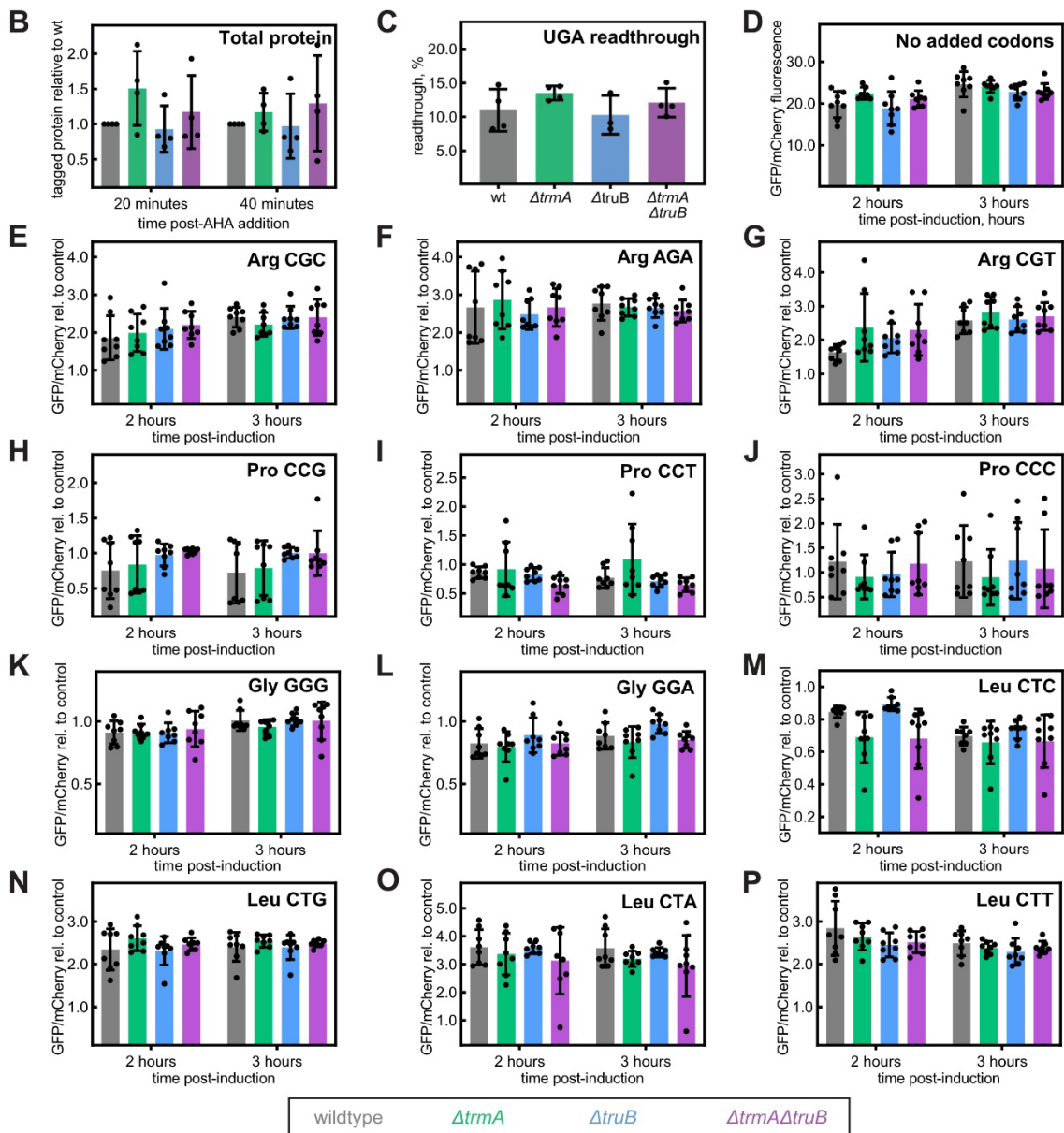
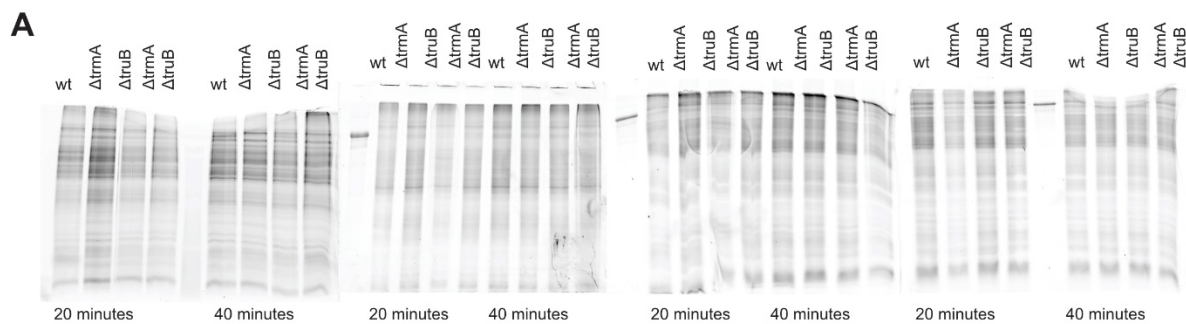
**Figure S4. Relative tRNA modification changes in the absence of *trmA* and/or *truB*.** (A) Mutation rate observed during MSR-seq at position 34 of tRNA<sup>Arg</sup><sub>ACG</sub>, indicating presence of the inosine modification. (B, C) Full, unedited gel images for two biological replicates (replicate 1, B; replicate 2, C) for tRNA<sup>Phe</sup> primer extension to detect acp<sup>3</sup>U47 modification. (D) To determine the relative acp<sup>3</sup>U47 content between strains, the reverse transcription stop corresponding to acp<sup>3</sup>U47 was compared to that for ms<sup>2</sup>i<sup>6</sup>A37.



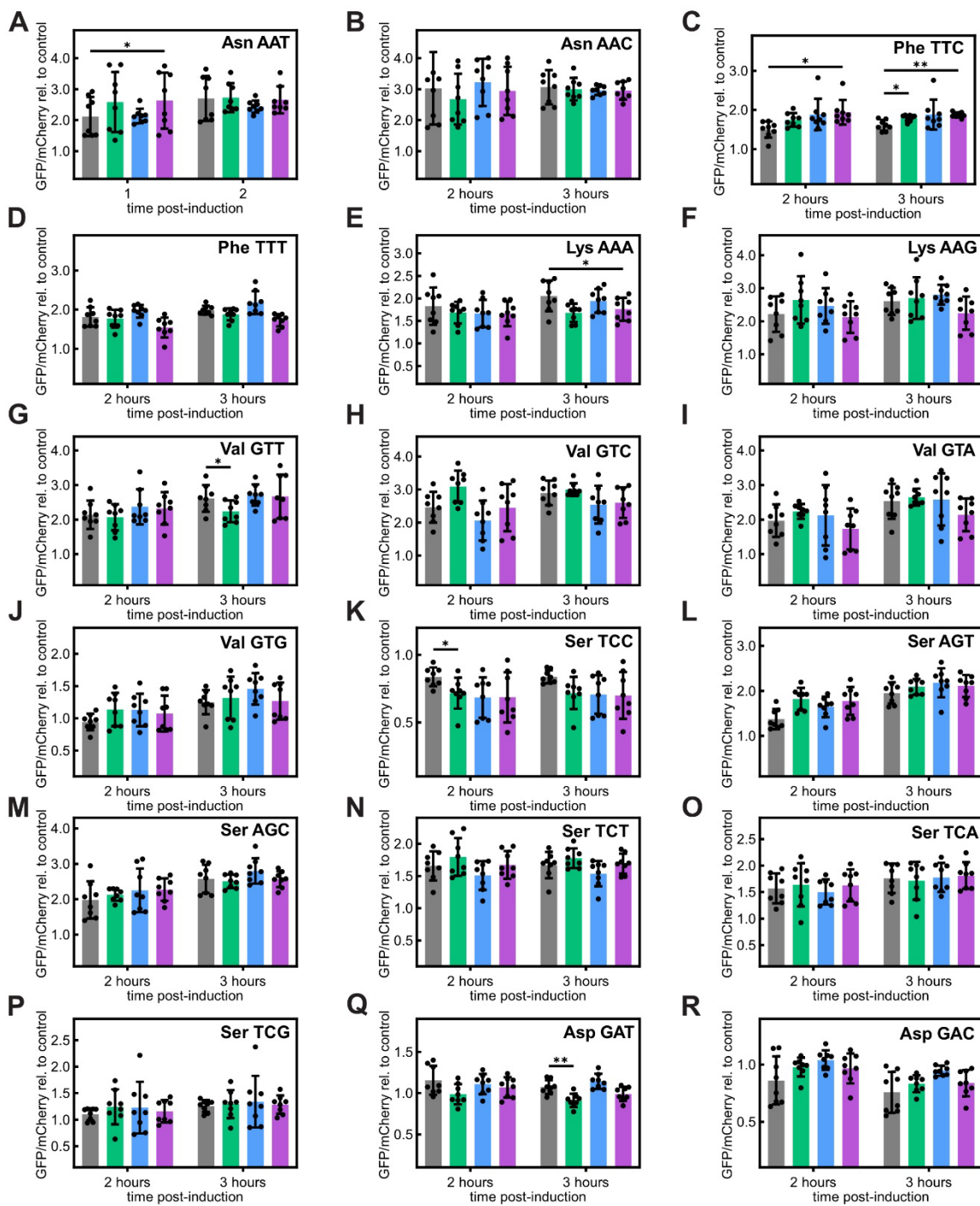
**Figure S5. APM Northern blotting to determine the levels of s<sup>4</sup>U8 in specific tRNAs.** In the presence of APM, thiolated tRNA migrates slowly (indicated by orange triangle) compared to the faster-migrating non-thiolated form (blue triangle). **(A)** Upon knockout of *trmA* and/or *truB*, no change in thiolation levels are identified within several tRNAs when *E. coli* strains are grown in LB media. **(B)** When *E. coli* is grown in LB supplemented with 2% (w/v) sodium formate, thiolation levels were found to be

increased in *trmA* and *truB* knockout strains compared to wildtype only for tRNA<sup>Asp</sup><sub>GTC</sub> (see Figure 2H). Two-three replicates were conducted for each experiment, as indicated in the figure.

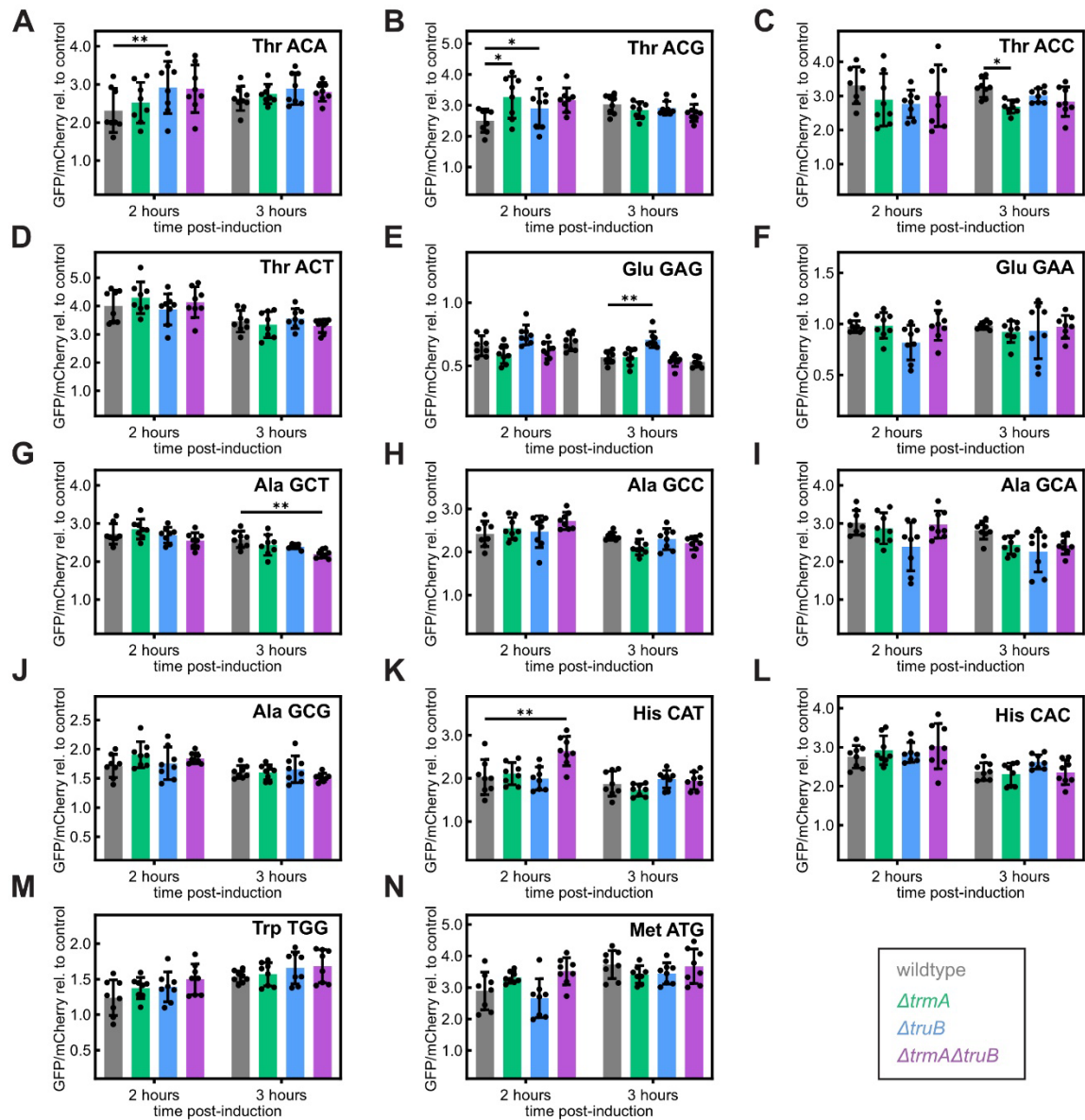




**Figure S6. Absence of TrmA and/or TruB does not affect global translation but disproportionately affects translation of specific codons (set 1).** **(A)** Original SDS-PAGEs detecting newly synthesized proteins within early logarithmic cells after 20 minutes and 40 minutes post labeling using the BONCAT pulse labeling assay in the  $\Delta trmA$ ,  $\Delta truB$ ,  $\Delta trmA\Delta truB$  and wild-type *E. coli* strains (n = 4 biological replicates for each strain). **(B)** Quantification of BONCAT gels shown in (A). **(C)** Proportion of UGA readthrough by Sec-tRNA<sup>Sec</sup> in the context of the *fdhF* SECIS element using a dual luciferase construct **(D to P)** The GFP reporter gene is preceded by four consecutive codons as indicated in the top right for each panel, and GFP expression is compared 2 and 3 hours after induction relative to mCherry expression encoded on the same plasmid. Codon-specific GFP translation is reported for the  $\Delta trmA$  (green),  $\Delta truB$  (blue),  $\Delta trmA\Delta truB$  (purple) and wild-type (grey) *E. coli* strains. In panel (B), a control is shown where no consecutive codons precede the GFP gene showing that general translation is not affected in the knockout strains.

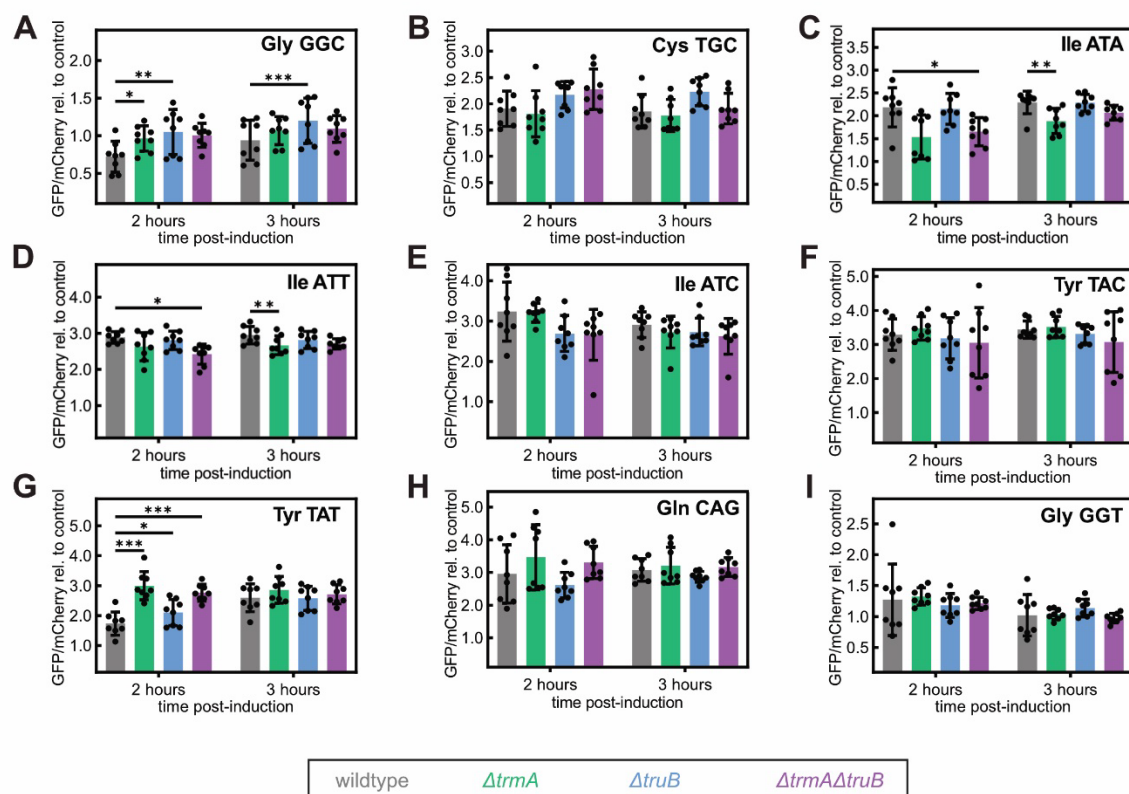


**Figure S7. Absence of TrmA and/or TruB disproportionately affects translation of specific codons (set 2).** The GFP reporter gene is preceded by four consecutive codons as indicated in the top right for each panel, and GFP expression is compared 2 and 3 hours after induction relative to mCherry expression encoded on the same plasmid. Codon-specific GFP translation is reported for the  $\Delta trmA$  (green),  $\Delta truB$  (blue),  $\Delta trmA\Delta truB$  (purple) and wild-type (grey) *E. coli* strains. Eight biological replicates were performed for each strain; \* indicates  $p < 0.05$ , \*\* indicates  $p < 0.01$ , and \*\*\* indicates  $p < 0.001$ .

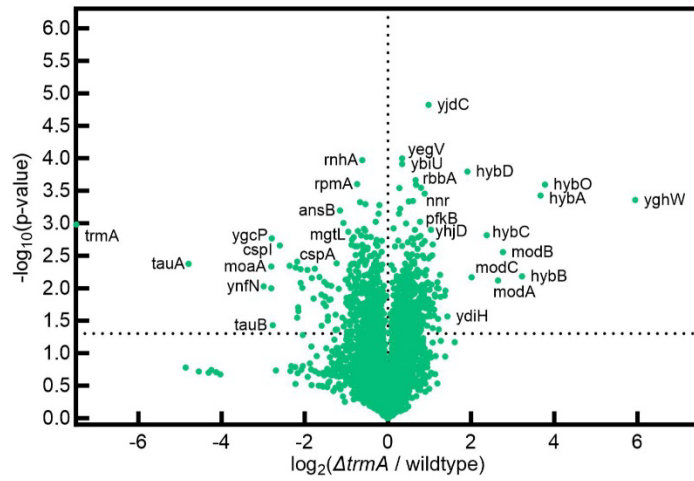
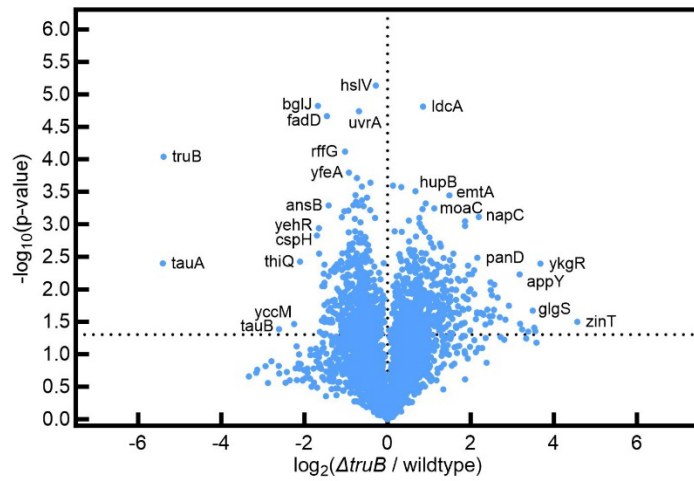
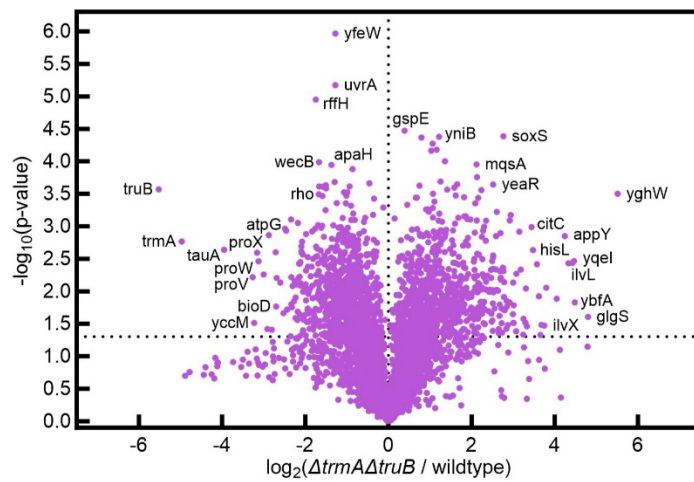


**Figure S8. Absence of TrmA and/or TruB disproportionately affects translation of specific codons (set 3).** The GFP reporter gene is preceded by four consecutive codons as indicated in the top right for each panel, and GFP expression is compared 2 and 3 hours after induction relative to mCherry expression encoded on the same plasmid. Codon-specific GFP translation is reported for the  $\Delta trmA$  (green),  $\Delta truB$  (blue),

$\Delta trmA\Delta truB$  (purple) and wild-type (grey) *E. coli* strains. Eight biological replicates were performed for each strain; \* indicates  $p < 0.05$ , \*\* indicates  $p < 0.01$ , and \*\*\* indicates  $p < 0.001$ .



**Figure S9. Absence of TrmA and/or TruB disproportionately affects translation of specific codons (set 4).** The GFP reporter gene is preceded by four consecutive codons as indicated in the top right for each panel, and GFP expression is compared 2 and 3 hours after induction relative to mCherry expression encoded on the same plasmid. Codon-specific GFP translation is reported for the  $\Delta trmA$  (green),  $\Delta truB$  (blue),  $\Delta trmA\Delta truB$  (purple) and wild-type (grey) *E. coli* strains. Eight biological replicates were performed for each strain; \* indicates  $p < 0.05$ , \*\* indicates  $p < 0.01$ , and \*\*\* indicates  $p < 0.001$ .

**A****B****C**



**Figure S10. Volcano plots showing the change in relative mRNA abundance between *E. coli* wildtype and  $\Delta trmA$  (A),  $\Delta truB$  (B), and  $\Delta trmA\Delta truB$  (C) strains.**

Horizontal line represents  $p = 0.05$ . Each data point is the average of three biological replicates.

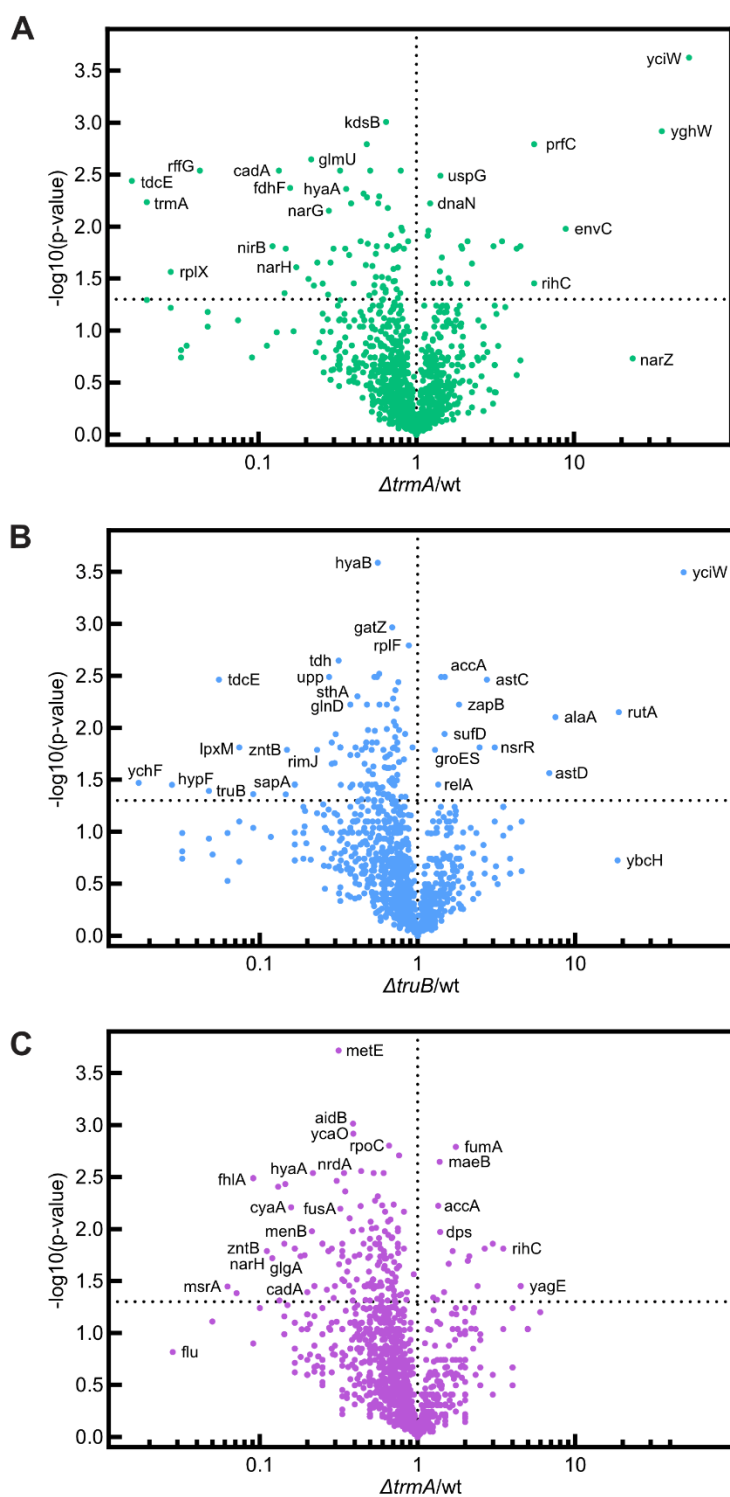


**Figure 11. Volcano plots showing the change in relative protein abundance**

between *E. coli* wildtype and  $\Delta trmA$  (A),  $\Delta truB$  (B), and  $\Delta trmA\Delta truB$  (C). Horizontal line represents  $p = 0.05$ . Each data point is the average of three biological replicates.

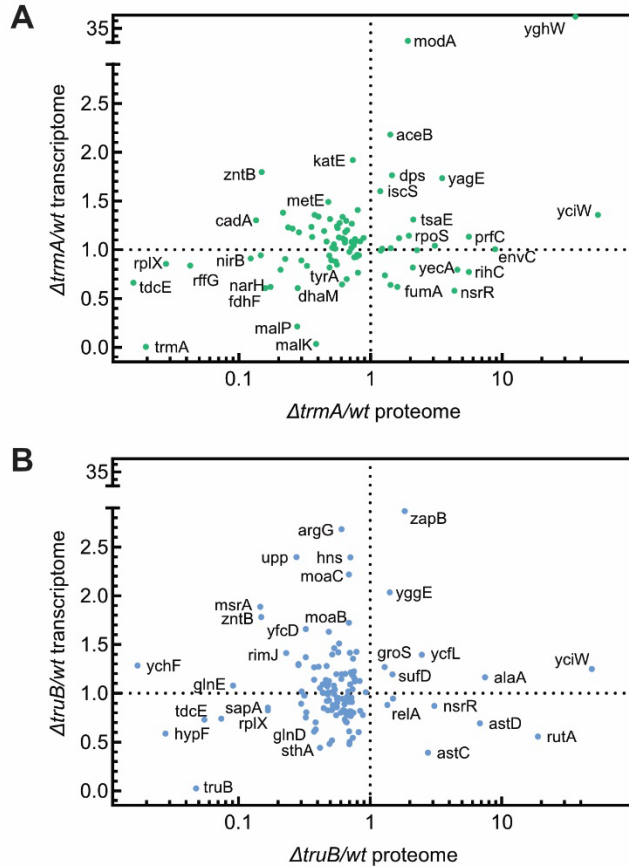
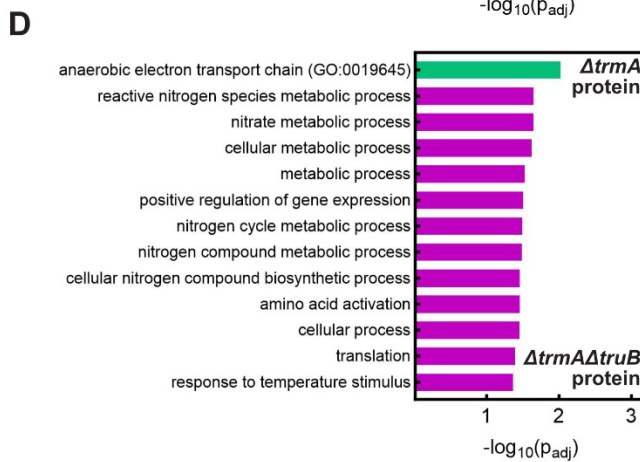
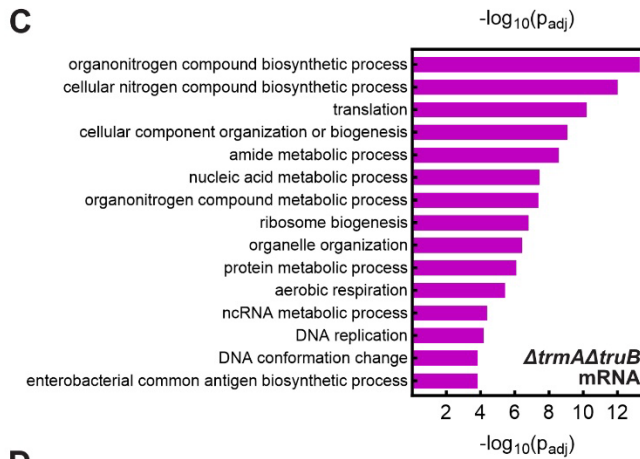
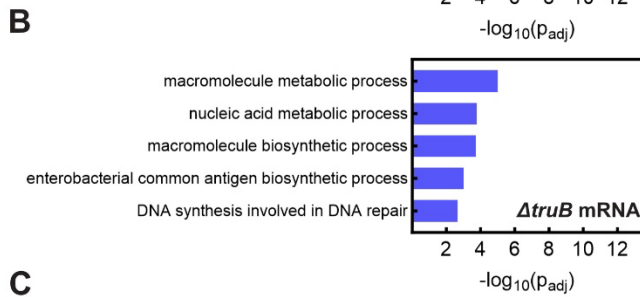
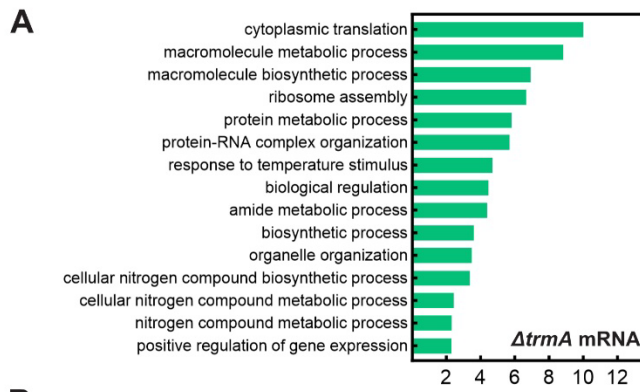
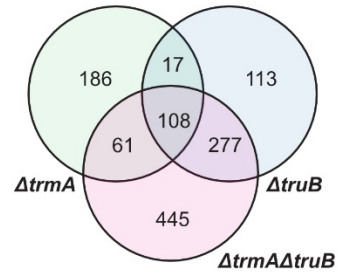


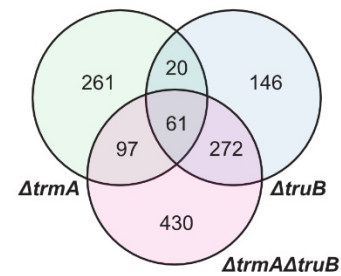
**Figure S12. Changes in gene expression in the single *trmA* (A) and *truB* (B) deletion strains.** Each data point represents a protein with a significantly ( $p < 0.05$ ) altered abundance within the knockout compared to wildtype, with fold protein change (knockout/wildtype) indicated on the x-axis. To address proteins that were not identified in any wildtype replicates (fold change = division by zero) or not identified in a knockout (fold change = 0), a small value (0.1) was added to each value. For each significantly altered protein, the respective mRNA fold change (knockout/wildtype) is indicated on the y-axis. Proteomics and transcriptomics experiments are the average of four and three biological replicates, respectively.



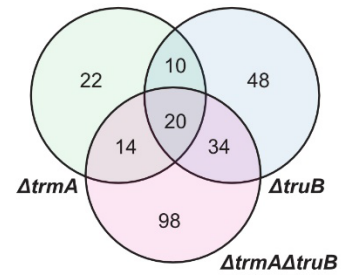
**E** Downregulated mRNAs ( $p < 0.05$ ):



**F** Upregulated mRNAs ( $p < 0.05$ ):



**G** Downregulated proteins ( $p < 0.05$ ):



**H** Upregulated proteins ( $p < 0.05$ ):

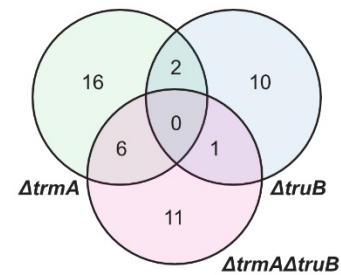


**Figure S13. Transcriptomic and proteomic changes in single and double *trmA/truB* knockout strains for datasets displayed in Fig. S11 and S12.** Gene ontology analysis for downregulated mRNAs in  $\Delta trmA$  (**A**),  $\Delta truB$  (**B**), and  $\Delta trmA\Delta truB$  (**C**) strains and for downregulated proteins within  $\Delta trmA$  and  $\Delta trmA\Delta truB$  strains (**D**). No gene ontology terms were found to be significantly enriched for downregulated proteins within the  $\Delta truB$  strain. Overlap between downregulated and upregulated mRNAs (**E, F**) and proteins (**G, H**) identified in each knockout strain.

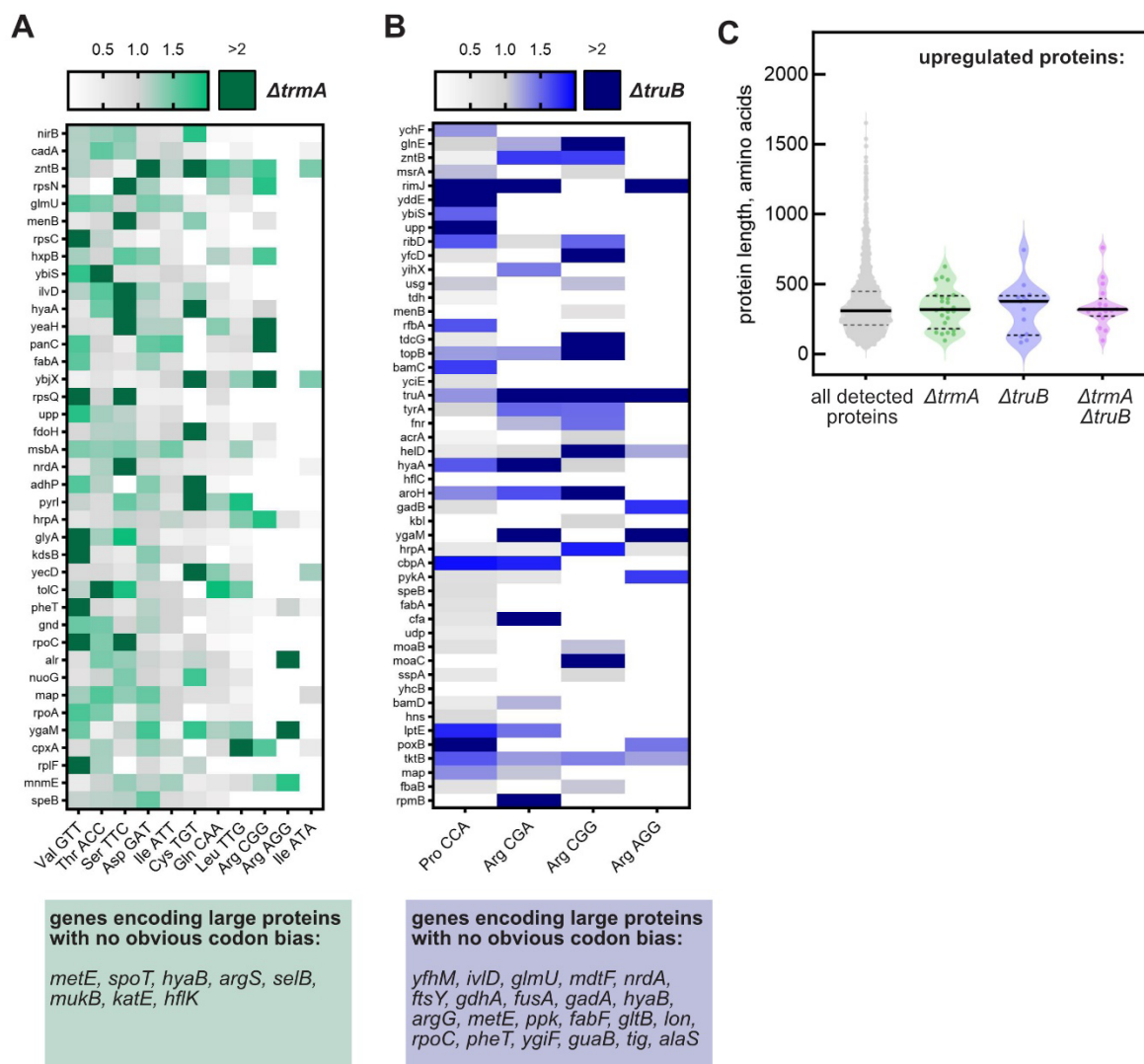


**Figure S14. Downregulated proteins within  $\Delta trmA$  and  $\Delta truB$  strains are enriched in poorly translated codons.** Relative codon frequencies compared to average codon usage for poorly translated codons within downregulated proteins with increased mRNA levels in **(A)**  $\Delta trmA$  and **(B)**  $\Delta truB$  single knockout strains. **(C)** Protein lengths (in amino acids) for each upregulated protein detected within  $\Delta trmA$  (green,  $n = 24$ ),  $\Delta truB$  (blue,  $n = 13$ ),  $\Delta trmA \Delta truB$  (purple,  $n = 17$ ) strains compared to the lengths of all proteins detected by mass-spectrometry (grey,  $n = 1951$ ). Solid lines represent median and dotted lines represent quartiles.

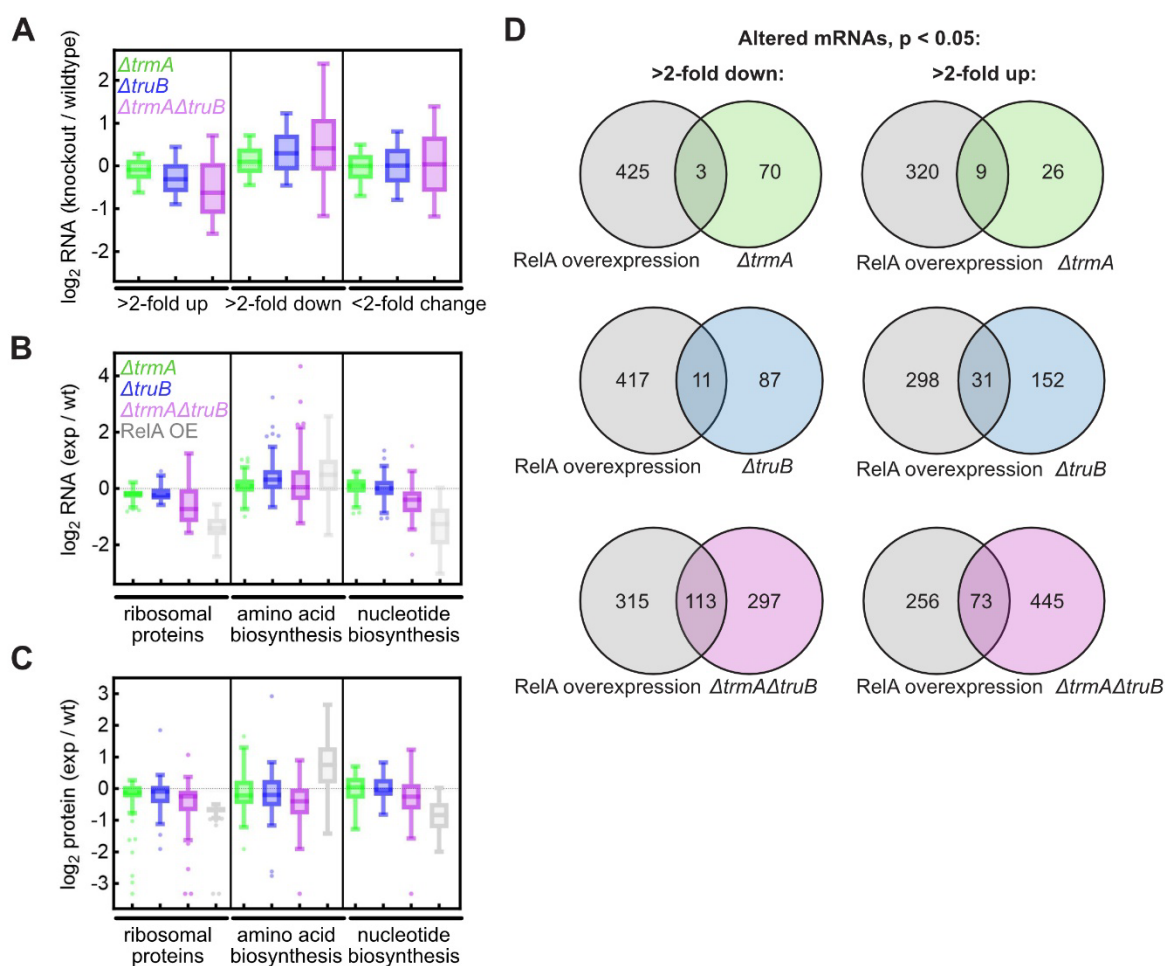


**Figure S15. Knockout of *trmA* and/or *truB* elicits a transcriptional response with some similar trends compared to, but distinct from, the bacterial stringent response.** (A) Log<sub>2</sub> fold change values for a set of mRNAs previously determined to be >2-fold up- (n = 316) or downregulated (n = 412) or non-responsive (<2-fold change, n = 3157) upon overexpression of RelA (22) within *ΔtrmA* (green), *ΔtruB* (blue), and *ΔtrmAΔtruB* (purple) strains compared to the wildtype strain. (B) Changes in relative mRNA abundances within *ΔtrmA* (green), *ΔtruB* (blue), and *ΔtrmAΔtruB* (purple) strains compared to the wildtype strain for genes encoding ribosomal proteins (n = 54) or genes encoding proteins classified by GO terms for amino acid biosynthesis (n = 102) or



nucleotide biosynthesis (n = 33). Grey box plots depict relative changes in mRNAs involved in these processes upon overexpression of RelA compared to a control strain (22). **(C)** Changes in relative protein abundances within  $\Delta trmA$  (green),  $\Delta truB$  (blue), and  $\Delta trmA\Delta truB$  (purple) strains compared to the wildtype strain for ribosomal proteins or proteins classified by GO terms for amino acid biosynthesis or nucleotide biosynthesis. **(D)** Overlap in mRNAs found to be both significantly ( $p < 0.05$ ) and >2-fold down- (left) or upregulated (right) within  $\Delta trmA$  (green),  $\Delta truB$  (blue), and  $\Delta trmA\Delta truB$  (purple) knockout strains compared to mRNAs >2-fold down-or upregulated upon overexpression of the RelA protein (22) indicates, although gene expression changes have similar trends as RelA overexpression for *trmA* and *truB* deletion strains, specific mRNA abundance changes are dissimilar. Lists of genes classified by each described GO terms were identified using the EcoCyc database (16).

## SI Table S1

**Table S1. Oligonucleotides used in this study (primers and Northern blotting probes)**

Name	Sequence
<i>trmA</i> left	5'- GAGCAATCCCTACAATCGCCGCGTACTTTAATTTTTCAGGATACATC ATGATTCCGGGGATCCGTCGACC-3'
<i>trmA</i> right	5'- GCCGGATGCTGGCGCATCCGGCATGGGTTTTACTTCGCGGTCAGTA ATACTGTAGGCTGGAGCTGCTTCG-3'
<i>truB</i> left	5'- CATGACGAAGAACGTCGTGTTAACCCGGACGACAGCAAGGAGGACT AATGATTCCGGGGATCCTTCGACC-3'
<i>truB</i> right	5'- AGCGACCTGTTATCGCAAGACGGTTAACATTACGCCGGGTATTCAAC CACTGTAGGCTGGAGCTGCTTCG-3'
Upstream <i>trmA</i>	5'-GGCTGTTCAAAACGGTTAGC-3'
Downstream <i>trmA</i>	5'-GCTGTTTAGCTCCATTGTGCC-3'
Upstream <i>truB</i>	5'-ATCAGGTCAACGTGAACAGC-3'
Downstream <i>truB</i>	5'-CGAGCAGTTTACGACGCTGAG-3'
Upstream <i>thil</i>	5'-TAACGCAGGCTTCGAGTTGC-3'
Downstream <i>thil</i>	5'-GCACTCTGCTGGTTGAAACC-3'
Upstream <i>tapT</i>	5'-CAGGTTGTGCGACATGCTTAATGG-3'
Downstream <i>tapT</i>	5'-AGTACCGGTCCGTTAAAGC-3'
k1 (kan internal forward)	5'-CAGTCATAGCCGAATAGCCT-3'
k2 (kan internal reverse)	5'-CGGTGCCCTGAATGAACTGC-3'
fluc-fdhF-rluc sense	5'-GTACTCCATGGATGGAAGACGCCAAAAACATAAAGAAAGGC-3'
fluc-fdhF-rluc antisense	5'-CATATGGATCCTTATTGTTCAATTTTTGAGAACTCGCTCAACG-3'

fdhF130-179UUC sense	5'-GCTCGTGTCTTCCACGGCCCATCGGTTGC-3'
fdhF130-179UUC antisense	5'-GCCGTGGAAGACACGAGCGCAGCAGTCAACG-3'
Cy5 tRNAPhe RT primer	5'-/Cy5/TGGTGCCCGGACTCGG-3'
tRNAPhe biotin	5'-/5Biosg/TGGTGCCCGGACTCGGAATCGAAC-3'
tRNAAsp biotin	5'-/5Biosg/TGGCGGAACGGACGGGACTCG-3'
tRNAIle(CAT) biotin	5'-/5Biosg/TGGTGGCCCCTGCTGGACTTGAACC-3'
tRNAArg(ACG) biotin	5'-/5Biosg/TGGTGCATCCGGGAGGATTTCG-3'
tRNAPro(CGG) biotin	5'-/5Biosg/TGGTCGGTGATAGAGGATTCTGAACCTC-3'
tRNAPro(UGG) biotin	5'-/5Biosg/TGGTCGGCGAGAGAGGATTCTGAAC-3'

## **Legends for Datasets S1 to S5**

**Dataset S1 (separate file).** Biolog phenotypic microarrays comparing cellular respiration over time for BW25113 wildtype and  $\Delta trmA\Delta truB$  strains. Yellow is overlap between the two strains, red is the BW25113 wildtype strain, and green is the  $\Delta trmA\Delta truB$  strain.

**Dataset S2 (separate file).** Averages and standard deviations for tRNA abundances determined using MSR-seq.

**Dataset S3 (separate file).** tRNA charging ratios for individual tRNAs in single (left) and double (right) knockout strains.

**Dataset S4 (separate file).** Raw mass spectrometry data and statistical analyses to compare the proteome between BW25113 wildtype,  $\Delta trmA$ ,  $\Delta truB$ ,  $\Delta trmA\Delta truB$  strains.

**Dataset S5 (separate file).** Codon counts and frequencies per 1000 for genes encoding downregulated proteins within the single  $\Delta trmA$  or  $\Delta truB$  and double  $\Delta trmA\Delta truB$  deletion strains.

## SI References

1. T. Baba *et al.*, Construction of Escherichia coli K-12 in-frame, single-gene knockout mutants: the Keio collection. *Mol Syst Biol* **2**, 2006.0008 (2006).
2. K. A. Datsenko, B. L. Wanner, One-step inactivation of chromosomal genes in Escherichia coli K-12 using PCR products. *Proc Natl Acad Sci U S A* **97**, 6640-6645 (2000).
3. B. R. Bochner, P. Gadzinski, E. Panomitros, Phenotype microarrays for high-throughput phenotypic testing and assay of gene function. *Genome Res* **11**, 1246-1255 (2001).
4. L. C. Keffer-Wilkes, G. R. Veerareddygar, U. Kothe, RNA modification enzyme TruB is a tRNA chaperone. *Proc Natl Acad Sci U S A* **113**, 14306-14311 (2016).
5. M. E. Evans, W. C. Clark, G. Zheng, T. Pan, Determination of tRNA aminoacylation levels by high-throughput sequencing. *Nucleic Acids Res* **45**, e133 (2017).
6. C. P. Watkins, W. Zhang, A. C. Wylder, C. D. Katanski, T. Pan, A multiplex platform for small RNA sequencing elucidates multifaceted tRNA stress response and translational regulation. *Nat Commun* **13**, 2491 (2022).
7. P. P. Chan, T. M. Lowe, GtRNAdb 2.0: an expanded database of transfer RNA genes identified in complete and draft genomes. *Nucleic Acids Res* **44**, D184-189 (2016).
8. S. K. Schultz, K. Meadows, U. Kothe, Molecular mechanism of tRNA binding by the Escherichia coli N7 guanosine methyltransferase TrmB. *J Biol Chem* **299**, 104612 (2023).
9. W. Zhang, R. Xu, Ź. Matuszek, Z. Cai, T. Pan, Detection and quantification of glycosylated queuosine modified tRNAs by acid denaturing and APB gels. *Rna* **26**, 1291-1298 (2020).
10. R. Heera *et al.*, Efficient extraction of small and large RNAs in bacteria for excellent total RNA sequencing and comprehensive transcriptome analysis. *BMC Res Notes* **8**, 754 (2015).
11. R. Hatzenpichler *et al.*, In situ visualization of newly synthesized proteins in environmental microbes using amino acid tagging and click chemistry. *Environ Microbiol* **16**, 2568-2590 (2014).
12. S. R. Khan *et al.*, Proteomic profile of aminoglutethimide-induced apoptosis in HL-60 cells: Role of myeloperoxidase and arylamine free radicals. *Chem Biol Interact* **239**, 129-138 (2015).
13. D. A. Kramer, M. A. Eldeeb, M. Wuest, J. Mercer, R. P. Fahlman, Proteomic characterization of EL4 lymphoma-derived tumors upon chemotherapy treatment reveals potential roles for lysosomes and caspase-6 during tumor cell death in vivo. *Proteomics* **17** (2017).
14. H. Mi *et al.*, Protocol Update for large-scale genome and gene function analysis with the PANTHER classification system (v.14.0). *Nat Protoc* **14**, 703-721 (2019).
15. F. Supek, M. Bošnjak, N. Škunca, T. Šmuc, REVIGO summarizes and visualizes long lists of gene ontology terms. *PLoS One* **6**, e21800 (2011).
16. P. D. Karp *et al.*, The EcoCyc Database (2023). *EcoSal Plus* **11**, eesp00022023 (2023).

17. P. Stothard, The sequence manipulation suite: JavaScript programs for analyzing and formatting protein and DNA sequences. *Biotechniques* **28**, 1102, 1104 (2000).
18. P. Rice, I. Longden, A. Bleasby, EMBOSS: the European Molecular Biology Open Software Suite. *Trends Genet* **16**, 276-277 (2000).
19. L. E. Leiva *et al.*, Oxidative stress strongly restricts the effect of codon choice on the efficiency of protein synthesis in Escherichia coli. *Front Microbiol* **13**, 1042675 (2022).
20. S. B. Kotini, F. Peske, M. V. Rodnina, Partitioning between recoding and termination at a stop codon-selenocysteine insertion sequence. *Nucleic Acids Res* **43**, 6426-6438 (2015).
21. R. T. Byrne, A. L. Konevega, M. V. Rodnina, A. A. Antson, The crystal structure of unmodified tRNAPhe from Escherichia coli. *Nucleic Acids Res* **38**, 4154-4162 (2010).
22. P. Sanchez-Vazquez, C. N. Dewey, N. Kitten, W. Ross, R. L. Gourse, Genome-wide effects on Escherichia coli transcription from ppGpp binding to its two sites on RNA polymerase. *Proc Natl Acad Sci U S A* **116**, 8310-8319 (2019).